Study of ^{89}Zr-Pembrolizumab PET/CT in Patients With Advanced-Stage Non–Small Cell Lung Cancer

Anna-Larissa N. Niemeijer[1], Daniela E. Oprea-Lager[2], Marc C. Huisman[2], Otto S. Hoekstra[2], Ronald Boellaard[2], Berlinda J. de Wit-van der Veen[3], Idris Bahce[1], Daniëlle J. Vugts[2], Guus A.M.S. van Dongen[2], Erik Thunnissen[4], Egbert F. Smit[1,5], and Adrianus J. de Langen[1,5]

[1]Department of Pulmonary Diseases, Cancer Center Amsterdam, Amsterdam University Medical Centers, Amsterdam, The Netherlands; [2]Department of Radiology and Nuclear Medicine, Cancer Center Amsterdam, Amsterdam University Medical Centers, Amsterdam, The Netherlands; [3]Department of Nuclear Medicine, NKI-AvL, Amsterdam, The Netherlands; [4]Department of Pathology, Cancer Center Amsterdam, Amsterdam University Medical Centers, Amsterdam, The Netherlands; and [5]Department of Thoracic Oncology, NKI-AvL, Amsterdam, The Netherlands

See an invited perspective on this article on page 359.

The tumor programmed death ligand 1 (PD-L1) proportion score is the current method for selecting non–small cell lung cancer (NSCLC) patients for single-agent treatment with pembrolizumab, a programmed cell death 1 (PD-1) monoclonal antibody. However, not all patients respond to therapy. Better understanding of in vivo drug behavior may help in the selection of patients who will benefit the most. **Methods:** NSCLC patients eligible for pembrolizumab monotherapy as first- or later-line therapy were enrolled. Patients received 2 injections of ^{89}Zr-pembrolizumab, 1 without a preceding dose of pembrolizumab and 1 with a preceding dose of 200 mg of pembrolizumab, directly before tracer injection. Up to 4 PET/CT scans were obtained after tracer injection. After imaging acquisition, patients were treated with 200 mg of pembrolizumab every 3 wk. Tumor uptake and tracer biodistribution were visually assessed and quantified as the SUV. Tumor tracer uptake was correlated with PD-1 and PD-L1 expression and response to pembrolizumab treatment. **Results:** Twelve NSCLC patients were included. One patient experienced grade 3 myalgia after tracer injection. ^{89}Zr-pembrolizumab was observed in the blood pool, liver, and spleen. Tracer uptake was visualized in 47.2% of 72 tumor lesions measuring BXP20 mm in the long-axis diameter, and substantial uptake heterogeneity was observed within and between patients. Uptake was higher in patients with a response to pembrolizumab treatment ($n = 3$) than in patients without a response ($n = 9$), although this finding was not statistically significant (median SUV_{peak}, 11.4 vs. 5.7; $P = 0.066$). No significant correlations were found with PD-L1 or PD-1 immunohistochemistry. **Conclusion:** ^{89}Zr-pembrolizumab injection was safe, with only 1 grade 3 adverse event—possibly immune-related—in 12 patients. ^{89}Zr-pembrolizumab tumor uptake was higher in patients with a response to pembrolizumab treatment but did not correlate with PD-L1 or PD-1 immunohistochemistry.

Key Words: NSCLC; immunotherapy; PET imaging

J Nucl Med 2022; 63:362–367
DOI: 10.2967/jnumed.121.261926

Immune checkpoint inhibitors have changed the treatment paradigm of advanced non–small cell lung cancer (NSCLC). However, identifying individual patients who will benefit from immune checkpoint inhibitors remains challenging. Better selection of patients will likely lead to higher response rates, fewer unnecessary toxicities, and reduced costs. The current method of selecting patients for single-agent treatment with pembrolizumab, a programmed cell death 1 (PD-1) monoclonal antibody, consists of scoring tumor programmed death ligand 1 (PD-L1) expression using immunohistochemistry. Although pembrolizumab monotherapy has been approved for the first- and second-line treatment of NSCLC patients with a PD-L1 tumor proportion score (TPS) of 1% or higher, only 28% of patients show a response to treatment, according to RECIST 1.1; the highest response rates were 40%–45% for patients with a TPS of greater than or equal to 50% (*1–4*). At the same time, approximately 10% of patients without tumor PD-L1 expression respond to treatment (*1*,*5*).

PET with radiolabeled antibodies visualizes and quantifies pharmacokinetics in vivo, which may help in the understanding of antibody behavior in blood and tissues (*6*). Previous research on NSCLC patients with radiolabeled immune checkpoint inhibitors revealed intra- and interpatient heterogeneity of tumor uptake for ^{89}Zr-nivolumab (PD-1) and ^{89}Zr-atezolizumab (PD-L1) (*7*,*8*). ^{89}Zr-atezolizumab uptake strongly correlated with a response, whereas ^{89}Zr-nivolumab uptake correlated with a lesional response but not an overall response. To our knowledge, studies of people with ^{89}Zr-labeled pembrolizumab have not been performed yet. Preclinical studies with ^{64}Cu- and ^{89}Zr-labeled pembrolizumab in mice and rats showed uptake in the spleen and liver and specific targeting of PD-1 (*9*,*10*). Although nivolumab and pembrolizumab are PD-1–blocking antibodies with structural similarities, they bind to different areas on the PD-1 receptor (*11–13*). In this feasibility study, we aimed to investigate whether the administration of ^{89}Zr-pembrolizumab is safe, to assess the biodistribution of ^{89}Zr-pembrolizumab, and to correlate the tracer uptake with PD-1 and PD-L1 immunohistochemistry and the response to pembrolizumab treatment.

MATERIALS AND METHODS

Patients

This study was conducted according to the Declaration of Helsinki. The institutional review board (Medical Ethics Committee of the Amsterdam

Received Jan. 11, 2021; revision accepted May 20, 2021.
For correspondence or reprints, contact Adrianus J. de Langen (j.d.langen@nki.nl).
Published online Jul. 16, 2021.

University Medical Centers [VU University Medical Center], Amsterdam, The Netherlands) approved this study, and all subjects signed a written informed consent form. The trial was registered at www.clinicaltrials.gov (Clinical Trials Identifier: NCT03065764). Twelve patients with advanced NSCLC eligible for pembrolizumab treatment were included in this multicenter trial.

Tumor Biopsies

Histologic tumor biopsies were obtained before the first ^{89}Zr-pembrolizumab injection and after the last line of systemic therapy, in case patients received prior therapy. Tumor tissue sections were stained with hematoxylin and eosin (H&E), PD-L1 (Dako PD-L1 IHC 22C3 pharmDx), and PD-1 (Cell Marque Corp. Clone NAT105 antibody). An experienced thoracic pathologist who was unaware of clinical information evaluated the slides. PD-L1 and PD-1 expression was measured as total (both tumor and immune cells) PD-L1 and PD-1 expression. In addition, tumor PD-L1 expression was scored as the percentage of tumor cells showing positive staining in the sample. PD-L1 was scored according to 22C3 scoring guidelines (*14*). PD-L1 and PD-1 were also scored according to the SP142 scoring system (IC0, IC1, IC2, IC3) (*15*), but still with the 22C3 antibody.

^{89}Zr-Pembrolizumab

^{89}Zr-pembrolizumab was produced in compliance with current good manufacturing practices at Amsterdam University Medical Centers [VU University Medical Center], Amsterdam, The Netherlands) according to validated procedures (*16–18*). Pembrolizumab was labeled with ^{89}Zr in an inert way to ensure that ^{89}Zr-pembrolizumab kinetics fully resembled the kinetics of unlabeled pembrolizumab (*19*,*20*). ^{89}Zr-pembrolizumab was produced as previously described with slight modifications (*19*). The production process is described in detail in the supplemental materials (supplemental materials are available at http://jnm.snmjournals.org).

Study Design

The study protocol consisted of 2 imaging series per patient, 1 without and 1 with a predose of unlabeled pembrolizumab (Supplemental Fig. 1). ^{89}Zr-pembrolizumab (37 MBq ± 10%; 2 mg of pembrolizumab) was intravenously injected on day 0. Static PET/CT scans from the skull vertex to the midthighs were performed 1 h and 3, 5, and 7 d after injection for the first 3 patients, whereas all other patients were scanned on days 3 and 6 after injection. On day 12, patients received an infusion of 200 mg of unlabeled pembrolizumab, followed within 2 h by a ^{89}Zr-pembrolizumab injection, to maximize the chance of representing therapeutic tumor targeting. A diagnostic CT scan of the thorax and upper abdomen and brain MRI were performed before the start of treatment. Pembrolizumab (200-mg flat dose) was administered every 3 wk until disease progression, unacceptable toxicity, or withdrawal of consent. Response assessment was performed with a diagnostic contrast-enhanced CT scan of the thorax and upper abdomen, with or without brain MRI (the latter only in case of pretreatment brain metastases), every 9 wk during treatment or more frequently if clinically indicated. RECIST 1.1 was used for assessment (*21*). Durable clinical benefit (DCB) was defined as a partial response or stable disease for greater than or equal to 6 mo.

PET Acquisitions

PET acquisitions were performed using a European Association of Nuclear Medicine Research Ltd.–calibrated Philips Ingenuity TF, Philips Big Bore, or Philips TF TOF PET/CT scanner (Philips Healthcare) at 10 min/bed position over the area containing the primary tumor and 5 min over the remaining bed positions. After this PET scan, a low-dose CT scan (50 mAs, 120 kV) was acquired for anatomic correlation and attenuation correction. Whole-body data were corrected for dead time, decay, scatter, and randoms and reconstructed with a matrix size of 144 × 144, 4-mm^3 voxels, and a time-of-flight iterative reconstruction method. The transaxial spatial resolution was approximately 5 mm full width at half maximum in the center of the field of view.

PET/CT Analyses

Reconstructed images were transferred to offline workstations for further analysis. Tumor accumulation was assessed by an experienced nuclear physician and described as focal or diffuse uptake exceeding the local background and incompatible with physiologic uptake. Volumes of interest (VOIs) were manually delineated on each scan using the Accurate tool (*22*). Liver, spleen, brain, lungs, and kidneys were manually delineated on each scan using the low-dose CT scan as an anatomic reference (*23*). Fixed VOIs were placed in the descending aorta to measure blood-pool activity and in the lumbar vertebrae to estimate the bone marrow activity concentration. Tracer uptake in all delineated VOIs was quantified semiquantitatively as the SUV. From each VOI, we derived the mean and peak activity concentrations (Bq/cm^3), normalized for body weight. SUV_{mean} is used to report organ tracer uptake, and SUV_{peak} is used for tumor lesions (*24*). To compare tracer uptake between imaging series 1 and 2, the percentage injected dose per gram (%ID/g) of tissue was calculated. To avoid partial-volume effects, only results for tumor lesions exceeding 20 mm in the long-axis diameter are reported.

Blood Samples

Blood samples for assessing ^{89}Zr-pembrolizumab concentrations were obtained at 5, 30, 60, and 120 min after injection for the first 3 patients. For the other patients, blood samples were drawn at 5 and 30 min after injection. Plasma and whole-blood concentrations were assessed by radioactivity measurements in a cross-calibrated γ-counter (Wallac Wizard 1480; PerkinElmer Inc.). The plasma activity concentration was calculated as the %ID/g.

Adverse Events

Adverse events were recorded from the initial signing of the informed consent form to the second full dose of pembrolizumab. The National Cancer Institute Common Terminology Criteria for Adverse Events version 4.0 were used (*25*).

Statistical Analysis

Statistical analysis was performed using SPSS statistics for Windows version 26.0 (IBM SPSS). The median SUV_{peak} of all delineated lesions (long-axis diameter of ≥20 mm) per patient were calculated and used to compare the median values of patients with a DCB and patients without a DCB. Because of the small patient numbers, PD-1 immunohistochemistry was dichotomized as "PD-1 low" (IC0 and IC1) and "PD-1 high" (IC2 and IC3). A Mann–Whitney–Wilcoxon rank sum test was performed to evaluate differences in SUV for a response and immunohistochemistry. Progression-free survival (PFS) was summarized using Kaplan–Meier plots. PFS was defined from the date the patient received the first pembrolizumab cycle to the date of radiologic progression or death (whichever occurred first). The median SUV_{peak} of the full cohort was used to stratify high uptake versus low uptake, and the log-rank test was used to compare the groups. Correlations between SUV_{peak} of tumor lesions on different scan days were calculated using the Spearman rank correlation coefficient. The Wilcoxon signed rank test and the Friedman test were performed for paired data (multiple groups). *P* values of less than 0.05 were considered statistically significant.

RESULTS

Patients

Twelve patients, 5 chemotherapy naive and 7 with progression after first- or second-line treatment, were enrolled (Supplemental Table 1). All patients had histopathologically confirmed lung

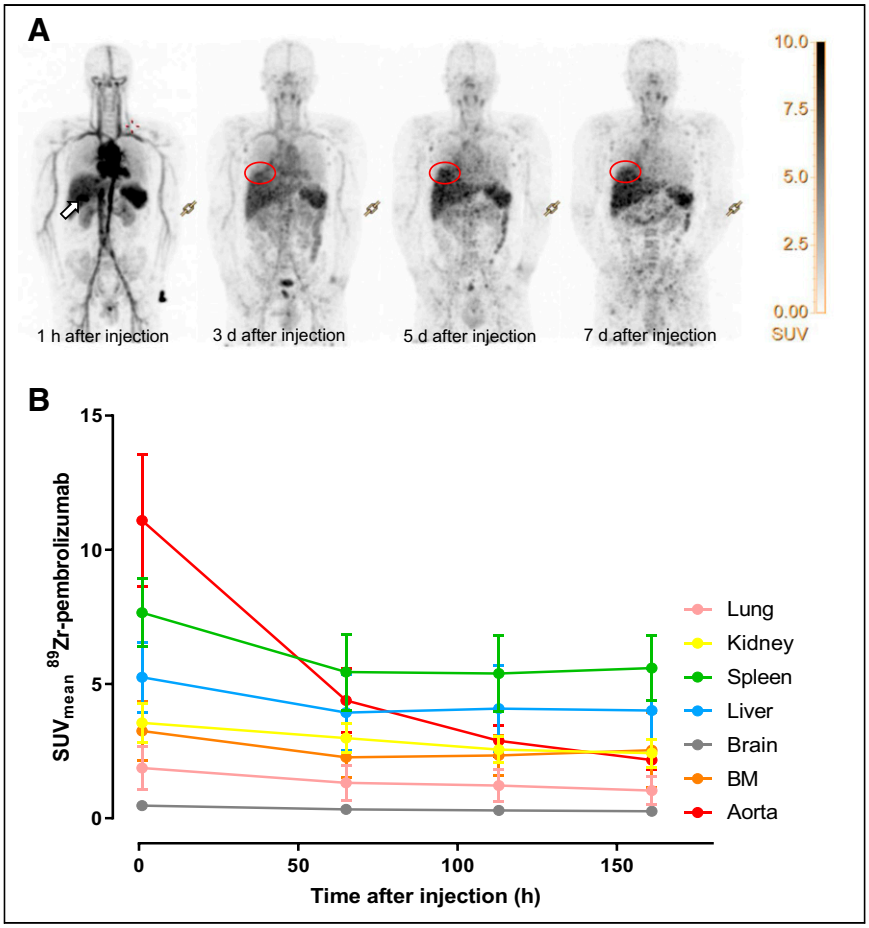

FIGURE 1. Biodistribution of ^{89}Zr-pembrolizumab. (A) Maximum-intensity-projection image of patient 1. White arrow indicates gallbladder. Red circle indicates primary tumor. (B) Tracer uptake per time point, measured as mean SUV_{mean} for first 3 patients at 1.1 ± 0.3, 65.8 ± 0.3, 113.2 ± 0.7, and 161.4 ± 0.81 h after injection. BM = bone marrow.

adenocarcinoma. Patients who were chemotherapy naive had higher PD-1 and PD-L1 expression rates than patients who received prior chemotherapy. Eight patients completed the full imaging series. For patients 2 and 3, scans were not performed at days 12 and 14, respectively, because of logistical problems. Patient 6 did not receive the second injection or treatment because of a large brain metastasis that required immediate treatment, and patient 7 refused to undergo the last PET/CT scan because of dyspnea. For patient 12, only a scan of the thorax could be obtained at days 6, 15, and 18 because of severe myalgia (grade III).

Safety

The most frequently reported adverse events were fatigue, anorexia, and dyspnea (Supplemental Table 2), most of which were disease related. In 1 patient, grade III anemia was observed, but the onset was before tracer injection. One patient experienced grade III myalgia after the first ^{89}Zr-pembrolizumab injection. This patient discontinued treatment after the first pembrolizumab cycle because of the myalgia and had progressive disease within 6 mo after the start of treatment.

Pharmacokinetics

To explore whether microdosing of the tracer (2 mg) could be used to image tumor uptake, we compared the %ID/g in plasma, in organs, and in tumor lesions between the first imaging acquisition (part 1) and the second imaging acquisition (part 2). Plasma clearance was slower for part 2 than for part 1 (Supplemental Fig. 2). Because of limited data, no statistical tests were performed. The concentration of pembrolizumab in the spleen was lower in part 2, suggesting that the spleen served as a "sink" (Supplemental Fig. 3).

For the other organs, no differences were observed in %ID/g between part 1 and part 2 for the first 3 patients (Supplemental Fig. 2). Remarkably, not all tumor lesions that were identified in part 1 could be assessed in part 2 (Supplemental Table 3). Nineteen tumor lesions could be identified in 10 patients at multiple time points in part 1, and 10 lesions were visible at multiple time points in part 2 (Supplemental Fig. 3). In 2 patients, %ID/g in the primary tumor was higher in part 2 than in part 1 (Supplemental Fig. 3). In the following paragraphs, only data for part 1 are shown.

Biodistribution of ^{89}Zr-Pembrolizumab

On the first PET/CT scan (performed 1 h after injection), ^{89}Zr-pembrolizumab uptake was observed in the blood pool, liver, spleen, and kidneys (Fig. 1A). In 2 of 3 patients (66.6%), the gallbladder was also visualized (Fig. 1A). Circulating ^{89}Zr-pembrolizumab in the blood pool was highest (SUV_{mean}, 11.5 ± 1.4) at 1 h after injection and decreased over time (SUV_{mean}, 4.6 ± 1.2, 3.0 ± 0.5, and 2.3 ± 0.6 on days 3, 5, and 7 after injection, respectively) (Figs. 1A and 1B). Uptake was high in the liver and spleen (SUV_{mean}, 3.9 ± 1.4 and 5.5 ± 1.4, respectively, on day 3 after injection) (Figs. 1A and 1B) and remained stable over time (liver: SUV_{mean}, 4.1 ± 1.6 on day 5 after injection and 4.0 ± 1.6 on day 7 after injection; spleen: SUV_{mean}, 5.4 ± 1.4 on day 5 after injection and 5.6 ± 1.2 on day 7 after injection). Intestinal uptake was variable (Fig. 1A), and low uptake was seen in the kidneys, bone marrow, non–tumor-bearing lung tissue, and brain (SUV_{mean}, 3.0 ± 0.6, 2.4 ± 0.5, 1.3 ± 0.7, and 0.4 ± 0.1, respectively, on day 3). In 8 of 12 patients, nonmalignant lymph nodes or adrenal glands showed low tracer uptake (examples are shown in Supplemental Fig. 4). In patient 1, an axillary lymph node (not suggestive of malignancy on an ^{18}F-FDG PET/CT scan) that showed low tracer uptake was biopsied. Histopathologic examination showed a high density of PD-1–positive lymphocytes in the secondary lymphoid follicles and no malignant cells. The adrenal glands of patient 3 were slightly enlarged at baseline but were not suggestive of metastases on the ^{18}F-FDG PET/CT scan, and the adrenal glands remained unchanged during follow-up CT scans.

Tumor Uptake

Overall, a total of 216 lesions from 12 patients were delineated on the pretreatment diagnostic CT scan (Table 1). Of these lesions, 140 (64.8%) had a diameter of less than 20 mm, 4 were difficult to measure because of atelectasis, and 72 (33%) had a diameter of greater than or equal to 20 mm. Sixty-two lesions (28.7%) were visible on

TABLE 1
Lesions on Diagnostic CT and ^{89}Zr-Pembrolizumab PET

Parameter	Value*
Total no. of lesions determined on diagnostic CT	216
Lesions < 20 mm	140 (64.8)
Lesions ≥ 20 mm	72 (33.3)
Measurement unreliable†	4 (1.8)
Lesions visible on PET/CT scan	62 (28.7)
Lesions < 20 mm	26 (18.6)
Lesions ≥ 20 mm	34 (47.2)
Measurement unreliable†	2
Lesions without uptake and > 20 mm	38
Brain	2
Lymph node	7
Lung	2
Bone	12
Liver	12
Adrenal gland	2
Soft tissue	1

*Values are numbers of lesions, with percentages in parentheses.
†Measurement of these lesions was unreliable because of atelectasis.

PET/CT. Of the 140 lesions with a diameter of less than 20 mm, 26 (18.6%) were visible on PET/CT on day 6 or 7. Of the 72 lesions with a long-axis diameter of greater than or equal to 20 mm, 34 (47.2%) were visible. Two lesions were difficult to measure. In all patients, at least 1 malignant lesion showed tracer uptake (median, 4.5; range, 2–17 [per patient]). For the first 3 patients, the median SUV_{peak} of tumor lesions increased over time from 4.9 (interquartile range, 3.5–6.6) on day 3 to 5.2 (interquartile range, 4.0–6.8) on day 5 to 5.9 (interquartile range, 4.0–7.0) on day 7 after injection (Fig. 2). There was no significant increase between day 5 and day 7 after injection ($P = 0.28$). Intralesional tracer distribution was heterogeneous (Fig. 3), and uptake patterns were variable (Figs. 4A–4D).

Of 4 patients who had brain metastases (38 lesions in total), 3 had been treated with (stereotactic) radiotherapy before the start of the present study (18/38 lesions) (Supplemental Table 4). Increased tracer uptake was observed in 2 patients (3 metastases): 1 patient had received whole-brain radiotherapy 9 mo before PET imaging (1 visible brain metastasis; long-axis diameter, 33.1 mm) (Fig. 4D), and 1 patient had not been irradiated before (2 visible brain metastases; long-axis diameters, 31.9 and 19.3 mm).

Response

For response evaluation, we reported the SUV_{peak} on day 6 or 7 because tumor uptake was the highest and blood-pool activity was the lowest, thus offering the best tumor-to-background ratio.

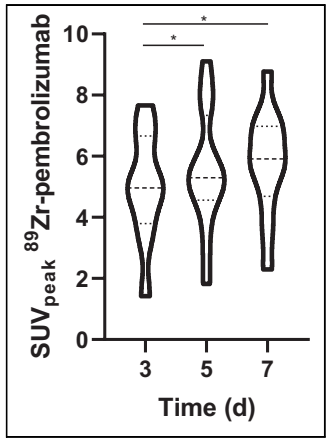

FIGURE 2. Median SUV_{peak} of all lesions for all patients.

Three patients had a DCB from pembrolizumab: 1 had a partial response according to RECIST 1.1, and 2 had stable disease. Patients with a DCB had a higher median tracer uptake, but this finding was not significant (median SUV_{peak}, 11.4 vs. 5.7; $P = 0.066$) (Fig. 5A). ^{89}Zr-pembrolizumab uptake increased with the best response category according to RECIST 1.1 ($P = 0.047$) (Fig. 5B). No partial response was observed in lesions with negative PET results. Patients with an SUV_{peak} higher than the median (SUV_{peak}, 6.7) had a longer PFS (median PFS, 25.0 wk) than those with an SUV_{peak} lower than the median (median PFS, 7.0 wk), although this finding was not significant ($P = 0.21$) (Fig. 5C).

Immunohistochemistry

Not all biopsied lesions ($n = 7/12$) showed ^{89}Zr-pembrolizumab uptake (Supplemental Table 5). PD-1 expression and tracer uptake were not correlated (the median SUV_{peak} were 7.9 for patients with high PD-1 expression and 7.4 for patients with low PD-1 expression; $P = 1.0$); neither were PD-L1 expression and tracer uptake (the median SUV_{peak} were 7.6 for patients with a TPS of <49% and 7.4 for patients with a TPS of ≥50%; $P = 0.72$) (Figs. 6A and 6B). Pretreatment PD-1 expression did not correlate with a response ($P = 0.41$), whereas pretreatment PD-L1 expression of greater than or equal to 50% did predict a response ($P = 0.049$).

DISCUSSION

This first-in-humans study of ^{89}Zr-pembrolizumab shows that injection of ^{89}Zr-pembrolizumab was well tolerated, with 1 possibly related adverse event. Tumor lesions could be visualized and quantified. For all patients, at least 1 tumor lesion showed tracer uptake after a single ^{89}Zr-pembrolizumab injection. Tumor uptake was heterogeneous within and between patients, and only 47.2% of the lesions with a long-axis diameter of greater than or equal to 20 mm showed uptake on the ^{89}Zr-pembrolizumab PET/CT scan.

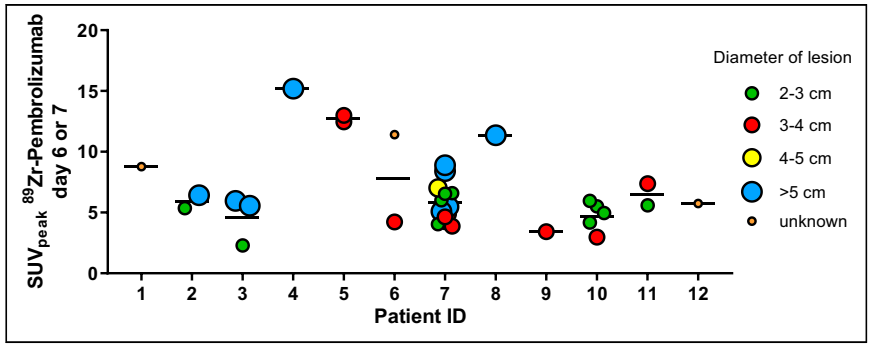

FIGURE 3. ^{89}Zr-pembrolizumab tumor uptake for all patients per delineated tumor.

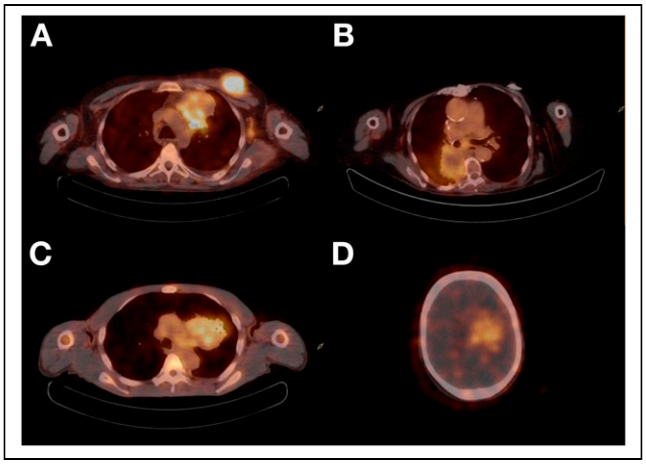

FIGURE 4. ^{89}Zr-pembrolizumab uptake patterns. (A) Heterogeneous uptake in paracardiac mass and homogeneous uptake in soft-tissue mass in left breast. (B) Rim uptake. (C) Heterogeneous uptake. (D) Uptake in brain metastasis.

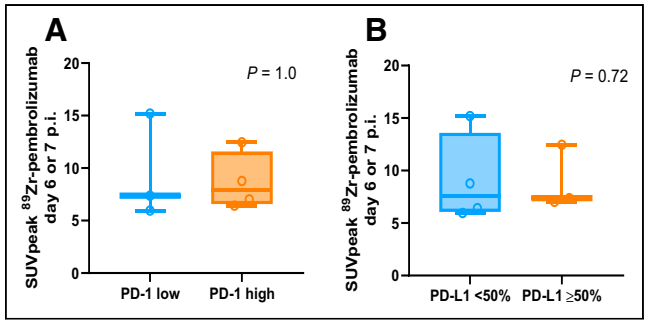

FIGURE 6. Relationship between tracer uptake and immunohistochemistry. (A) Correlation between SUV_{peak} and PD-1 expression of biopsied lesion. (B) Correlation between SUV_{peak} and PD-L1 expression of biopsied lesion. p.i. = postinjection.

All patients (except patient 6) underwent 2 imaging acquisitions, 1 without a predose of unlabeled pembrolizumab and 1 with a predose. Plasma clearance was slower when the predose was used. We observed lower tracer uptake in the spleen in part 2 than in part 1, suggesting that the predose saturated the PD-1 receptors in the spleen. In part 2 (with coinjection of a predose), only 10 lesions could be delineated in the first 3 patients, whereas 19 lesions could be delineated in these patients in part 1. We assume that a predose of 200 mg (flat dose of pembrolizumab) occupied most available PD-1 receptors, causing a loss of signal. Recently, a flow cytometry study in patients treated with pembrolizumab showed receptor occupancy on peripheral mononuclear blood cells at the end of the first infusion of 88%–100%, depending on cell type (*26*). Unfortunately, because of our limited data, we cannot determine an "optimal predose" of unlabeled pembrolizumab.

The biodistribution of ^{89}Zr-pembrolizumab was comparable to that observed in previous NSCLC studies with ^{89}Zr-labeled immune checkpoint inhibitors. High uptake was seen in the liver (likely because of tracer catabolism), the spleen (likely because of binding to PD-1 receptors on lymphocytes and dendritic cells, abundantly present in the spleen), and nonmalignant lymph nodes (*7*,*8*). PD-1 is expressed on a variety of immune cells, including activated and exhausted $CD8^+$ T cells, B cells, myeloid dendritic cells, and monocytes; in fact, most patients showed ^{89}Zr-pembrolizumab uptake in nonmalignant lymph nodes (*27*). Recent preclinical imaging studies with ^{89}Zr-pembrolizumab in mice and monkeys also reported high uptake in lymphoid tissues (*28*,*29*). Variable uptake was observed in the intestines, probably because of excretion. In none of the patients included in the present study was colitis observed during pembrolizumab treatment. Low uptake was observed in the kidneys, adrenal glands, bone marrow, lungs, and central nervous system, suggesting that this tracer has a beneficial profile for imaging lung cancer patients. In the present study, we observed tracer uptake in some brain metastases. Since most brain metastases were pretreated with radiotherapy and small in size (<20 mm), these factors could have contributed to the absence of tracer accumulation in several of these lesions.

Tracer uptake in nonmalignant lymph nodes is regarded as specific uptake. Lymph nodes are known for their role in the immune defense to pathogens, and tumor-draining lymph nodes are needed to engage an optimal antitumor immune response (*30*,*31*). Nonmalignant lymph nodes are known to contain PD-1–expressing immune cells (*27*). One lymph node not suggestive of malignant involvement was biopsied because it showed substantial ^{89}Zr-pembrolizumab uptake, and immunohistochemistry did indeed show high PD-1 expression in the follicles. Whether PD-1 expression in lymph nodes is necessary to obtain a response remains uncertain. In 1 patient, ^{89}Zr-pembrolizumab uptake exceeded the local background in benign adrenal glands. Lymphocytic infiltration of the adrenal gland has been described (*32*).

^{89}Zr-pembrolizumab uptake was higher in responding patients than in nonresponding patients, although this finding was not significant. Tumor uptake of ^{89}Zr-pembrolizumab increased with the best tumor response category according to RECIST 1.1. Similar findings were observed for anti–PD-L1 ^{89}Zr-atezolizumab PET/CT (*8*). We did observe that negative lesions on ^{89}Zr-pembrolizumab PET did not have a response to treatment, supporting our hypothesis that there is a link between uptake and response.

We were not able to find a correlation between PD-1 expression and ^{89}Zr-pembrolizumab uptake. Heterogeneity between surgical specimens and biopsies is well known and could account for the difference in tracer uptake and PD-1 expression in a small tumor biopsy (*33*,*34*). This possibility is further supported by the observation that ^{89}Zr-pembrolizumab tracer uptake was heterogeneous both within and between tumor lesions.

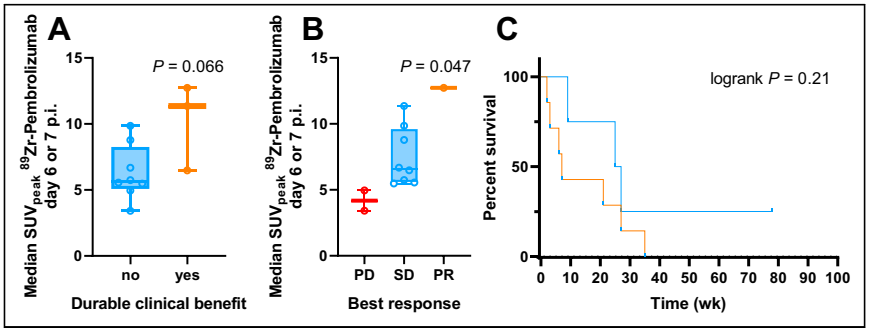

FIGURE 5. Relationship between tracer uptake and response. (A) Median tracer uptake of all lesions > 20 mm for responders and nonresponders. (B) Median tracer uptake per best RECIST response category. (C) Progression-free survival curve according to median SUV_{peak} (blue, above median SUV_{peak} of 6.7; orange, below median SUV_{peak}). p.i. = postinjection.

CONCLUSION

The present study shows that ^{89}Zr-pembrolizumab PET/CT imaging in patients with NSCLC is safe and feasible. In this limited dataset, we found that ^{89}Zr-pembrolizumab tracer uptake showed a nonsignificant correlation with a response to pembrolizumab treatment. Further research is needed to investigate the value of ^{89}Zr-pembrolizumab as a stand-alone biomarker or as adjunct information for tumor PD-L1 expression determined by immunohistochemistry.

DISCLOSURE

We received a research grant for the implementation of this study from Merck Sharpe & Dohme (MSD). MSD was not involved in the study design, data collection, analysis and interpretation of the data, or the writing of this report. No other potential conflict of interest relevant to this article was reported.

KEY POINTS

QUESTION: The aims of this study were to investigate whether the administration of ^{89}Zr-pembrolizumab was safe, to assess the biodistribution of ^{89}Zr-pembrolizumab, and to correlate the tracer uptake with PD-1 and PD-L1 immunohistochemistry and response to pembrolizumab treatment.

PERTINENT FINDINGS: In this feasibility study, we observed that ^{89}Zr-pembrolizumab uptake was safe and that it was higher in patients with a response (SUV_{peak}, 11.4) than in patients without a response (SUV_{peak}, 5.7), although this finding was not statistically significant.

IMPLICATIONS FOR PATIENT CARE: Further research is needed to investigate whether ^{89}Zr-pembrolizumab can be used as a biomarker.

REFERENCES

1. Garon EB, Rizvi NA, Hui R, et al. Pembrolizumab for the treatment of non-small-cell lung cancer. *N Engl J Med.* 2015;372:2018–2028.
2. Herbst RS, Baas P, Kim DW, et al. Pembrolizumab versus docetaxel for previously treated, PD-L1-positive, advanced non-small-cell lung cancer (KEYNOTE-010): a randomised controlled trial. *Lancet.* 2016;387:1540–1550.
3. Mok TSK, Wu YL, Kudaba I, et al. Pembrolizumab versus chemotherapy for previously untreated, PD-L1-expressing, locally advanced or metastatic non-small-cell lung cancer (KEYNOTE-042): a randomised, open-label, controlled, phase 3 trial. *Lancet.* 2019;393:1819–1830.
4. Reck M, Rodriguez-Abreu D, Robinson AG, et al. Pembrolizumab versus chemotherapy for PD-L1-positive non-small-cell lung cancer. *N Engl J Med.* 2016;375:1823–1833.
5. Shukuya T, Carbone DP. Predictive markers for the efficacy of anti-PD-1/PD-L1 antibodies in lung cancer. *J Thorac Oncol.* 2016;11:976–988.
6. Van Dongen GA, Huisman MC, Boellaard R, et al. ^{89}Zr-immuno-PET for imaging of long circulating drugs and disease targets: why, how and when to be applied? *Q J Nucl Med Mol Imaging.* 2015;59:18–38.
7. Niemeijer AN, Leung D, Huisman MC, et al. Whole body PD-1 and PD-L1 positron emission tomography in patients with non-small-cell lung cancer. *Nat Commun.* 2018;9:4664.
8. Bensch F, van der Veen EL, Lub-de Hooge MN, et al. ^{89}Zr-atezolizumab imaging as a non-invasive approach to assess clinical response to PD-L1 blockade in cancer. *Nat Med.* 2018;24:1852–1858.
9. England CG, Ehlerding EB, Hernandez R, et al. Preclinical pharmacokinetics and biodistribution studies of ^{89}Zr-labeled pembrolizumab. *J Nucl Med.* 2017;58:162–168.
10. Natarajan A, Patel CB, Habte F, Gambhir SS. Dosimetry prediction for clinical translation of ^{64}Cu-pembrolizumab immunoPET targeting human PD-1 expression. *Sci Rep.* 2018;8:633.
11. Fessas P, Lee H, Ikemizu S, Janowitz T. A molecular and preclinical comparison of the PD-1-targeted T-cell checkpoint inhibitors nivolumab and pembrolizumab. *Semin Oncol.* 2017;44:136–140.
12. Na Z, Yeo SP, Bharath SR, et al. Structural basis for blocking PD-1-mediated immune suppression by therapeutic antibody pembrolizumab. *Cell Res.* 2017;27:147–150.
13. Tan S, Zhang H, Chai Y, et al. An unexpected N-terminal loop in PD-1 dominates binding by nivolumab. *Nat Commun.* 2017;8:14369.
14. PD-L1 IHC 22C3 pharmDx Interpretation Manual – NSCLC. https://www.agilent.com/cs/library/usermanuals/public/29158_pd-l1-ihc-22C3-pharmdx-nsclc-interpretation-manual.pdf. Accessed November 8, 2021.
15. Herbst RS, Soria JC, Kowanetz M, et al. Predictive correlates of response to the anti-PD-L1 antibody MPDL3280A in cancer patients. *Nature.* 2014;515:563–567.
16. Jauw YW, Menke-van der Houven van Oordt CW, Hoekstra OS, et al. Immunopositron emission tomography with zirconium-89-labeled monoclonal antibodies in oncology: what can we learn from initial clinical trials? *Front Pharmacol.* 2016;7:131.
17. Verel I, Visser GW, Boellaard R, et al. Quantitative ^{89}Zr immuno-PET for in vivo scouting of ^{90}Y-labeled monoclonal antibodies in xenograft-bearing nude mice. *J Nucl Med.* 2003;44:1663–1670.
18. Perk LR, Vosjan MJ, Visser GW, et al. *p*-Isothiocyanatobenzyl-desferrioxamine: a new bifunctional chelate for facile radiolabeling of monoclonal antibodies with zirconium-89 for immuno-PET imaging. *Eur J Nucl Med Mol Imaging.* 2010;37:250–259.
19. Vosjan MJ, Perk LR, Visser GW, et al. Conjugation and radiolabeling of monoclonal antibodies with zirconium-89 for PET imaging using the bifunctional chelate *p*-isothiocyanatobenzyl-desferrioxamine. *Nat Protoc.* 2010;5:739–743.
20. Cohen R, Vugts DJ, Stigter-van Walsum M, Visser GW, van Dongen GA. Inert coupling of IRDye800CW and zirconium-89 to monoclonal antibodies for single- or dual-mode fluorescence and PET imaging. *Nat Protoc.* 2013;8:1010–1018.
21. Eisenhauer EA, Therasse P, Bogaerts J, et al. New response evaluation criteria in solid tumours: revised RECIST guideline (version 1.1). *Eur J Cancer.* 2009;45:228–247.
22. Frings V, van Velden FH, Velasquez LM, et al. Repeatability of metabolically active tumor volume measurements with FDG PET/CT in advanced gastrointestinal malignancies: a multicenter study. *Radiology.* 2014;273:539–548.
23. Boellaard RHO, Lammertsma AA. Software tools for standardized analysis of FDG whole-body studies in multicenter trials [abstract]. *J Nucl Med.* 2008;49:159P.
24. Lodge MA, Chaudhry MA, Wahl RL. Noise considerations for PET quantification using maximum and peak standardized uptake value. *J Nucl Med.* 2012;53:1041–1047.
25. National Cancer Institute. Common Terminology Criteria for Adverse Events (CTCAE) version 4.0. Bethesda, MD: National Cancer Institute, National Institutes of Health, U.S. Department of Health and Human Services; 2009.
26. Pluim D, Ros W, Miedema IHC, Beijnen JH, Schellens JHM. Multiparameter flow cytometry assay for quantification of immune cell subsets, PD-1 expression levels and PD-1 receptor occupancy by nivolumab and pembrolizumab. *Cytometry A.* 2019;95:1053–1065.
27. Keir ME, Butte MJ, Freeman GJ, Sharpe AH. PD-1 and its ligands in tolerance and immunity. *Annu Rev Immunol.* 2008;26:677–704.
28. van der Veen EL, Giesen D, Pot-de Jong L, Jorritsma-Smit A, De Vries EGE, Lub-de Hooge MN. ^{89}Zr-pembrolizumab biodistribution is influenced by PD-1-mediated uptake in lymphoid organs. *J Immunother Cancer.* 2020;8:e000938.
29. Li W, Wang Y, Rubins D, et al. PET/CT imaging of ^{89}Zr-*N*-sucDf-pembrolizumab in healthy cynomolgus monkeys. *Mol Imaging Biol.* 2021;23:250–259.
30. Fransen MF, Schoonderwoerd M, Knopf P, et al. Tumor-draining lymph nodes are pivotal in PD-1/PD-L1 checkpoint therapy. *JCI Insight.* 2018;3:e124507.
31. Spitzer MH, Carmi Y, Reticker-Flynn NE, et al. Systemic immunity is required for effective cancer immunotherapy. *Cell.* 2017;168:487–502.
32. Hayashi Y, Hiyoshi T, Takemura T, Kurashima C, Hirokawa K. Focal lymphocytic infiltration in the adrenal cortex of the elderly: immunohistological analysis of infiltrating lymphocytes. *Clin Exp Immunol.* 1989;77:101–105.
33. Ilie M, Long-Mira E, Bence C, et al. Comparative study of the PD-L1 status between surgically resected specimens and matched biopsies of NSCLC patients reveal major discordances: a potential issue for anti-PD-L1 therapeutic strategies. *Ann Oncol.* 2016;27:147–153.
34. McLaughlin J, Han G, Schalper KA, et al. Quantitative assessment of the heterogeneity of PD-L1 expression in non-small-cell lung cancer. *JAMA Oncol.* 2016;2:46–54.